

Export productivity and carbonate accumulation in the Pacific Basin at the transition from a greenhouse to icehouse climate (late Eocene to early Oligocene)

Elizabeth Griffith,^{1,2} Michael Calhoun,¹ Ellen Thomas,³ Kristen Averyt,^{1,4} Andrea Erhardt,¹ Timothy Bralower,⁵ Mitch Lyle,⁶ Annette Olivarez-Lyle,⁶ and Adina Paytan¹

Received 18 January 2010; revised 21 April 2010; accepted 7 May 2010; published 3 September 2010.

[1] The late Eocene through earliest Oligocene (40–32 Ma) spans a major transition from greenhouse to icehouse climate, with net cooling and expansion of Antarctic glaciation shortly after the Eocene/Oligocene (E/O) boundary. We investigated the response of the oceanic biosphere to these changes by reconstructing barite and CaCO₃ accumulation rates in sediments from the equatorial and North Pacific Ocean. These data allow us to evaluate temporal and geographical variability in export production and CaCO₃ preservation. Barite accumulation rates were on average higher in the warmer late Eocene than in the colder early Oligocene, but cool periods within the Eocene were characterized by peaks in both barite and CaCO₃ accumulation in the equatorial region. We infer that climatic changes not only affected deep ocean ventilation and chemistry, but also had profound effects on surface water characteristics influencing export productivity. The ratio of CaCO₃ to barite accumulation rates, representing the ratio of particulate inorganic C accumulation to C_{org} export, increased dramatically at the E/O boundary. This suggests that long-term drawdown of atmospheric CO₂ due to organic carbon deposition to the seafloor decreased, potentially offsetting decreasing pCO₂ levels and associated cooling. The relatively larger increase in CaCO₃ accumulation compared to export production at the E/O suggests that the permanent deepening of the calcite compensation depth (CCD) at that time stems primarily from changes in deep water chemistry and not from increased carbonate production.

Citation: Griffith, E., M. Calhoun, E. Thomas, K. Averyt, A. Erhardt, T. Bralower, M. Lyle, A. Olivarez-Lyle, and A. Paytan (2010), Export productivity and carbonate accumulation in the Pacific Basin at the transition from a greenhouse to icehouse climate (late Eocene to early Oligocene), *Paleoceanography*, 25, PA3212, doi:10.1029/2010PA001932.

1. Introduction

[2] Oceanic export productivity and carbon (C) burial are among the major forcing mechanisms of naturally occurring C sequestration, and thus play an important role in the global C cycle [e.g., Anderson *et al.*, 1990; Marinov and Sarmiento, 2004]. Accordingly, it has been postulated that changes in productivity, calcium carbonate (CaCO₃) to organic C (C_{org}) export ratio (CaCO₃:C_{org}, also called ‘rain ratio’), and burial efficiency have had profound effects on the partitioning of C between oceanic, atmospheric, and terrestrial reservoirs [e.g.,

Lyle *et al.*, 2008], influencing the partial pressure of atmospheric carbon dioxide (pCO₂), thus global climate. The Pacific Ocean, comprising half of the world’s surface ocean at present, and much more in the Eocene (ODSN plate reconstruction service, <http://www.geo-guide.de/cgi-bin/ssgfi/anzeige.pl?db=geo&nr=001109&ew=SSGFI>), is especially important for understanding global biogeochemical cycles and feedback between oceanic processes and climate, because of its large role in ocean export productivity and capacity for nutrient storage.

[3] The late Eocene and in particular the Eocene/Oligocene (E/O) transition was a period of considerable global climatic, biotic, and oceanographic change [e.g., Kennett and Stott, 1990; Bralower *et al.*, 1995; Diester-Haass and Zahn, 1996, 2001; Bohaty and Zachos, 2003; Coxall *et al.*, 2005; Miller *et al.*, 2005a; Thomas, 2007; Zanazzi *et al.*, 2007; Katz *et al.*, 2008; Lear *et al.*, 2008; Merico *et al.*, 2008; Bohaty *et al.*, 2009; Eldrett *et al.*, 2009; Liu *et al.*, 2009]. Starting at about 50 Ma, Earth’s climate began a transition from “greenhouse” to “icehouse” conditions, with cooling of the high latitudes and subsequently deep waters, as indicated by compilations of the benthic oxygen isotope record reconstructed from marine carbonates [e.g., Miller *et al.*, 1987, 2005a; Zachos *et al.*, 2001; Cramer *et al.*, 2009]. Cooling

¹Institute of Marine Sciences, University of California, Santa Cruz, California, USA.

²Department of Geology, Kent State University, Kent, Ohio, USA.

³Department of Earth and Environmental Sciences, Wesleyan University, Middletown, Connecticut, USA.

⁴NOAA Earth System Research Laboratory, University of Colorado at Boulder, Boulder, Colorado, USA.

⁵Department of Geosciences, Pennsylvania State University, University Park, Pennsylvania, USA.

⁶Department of Oceanography, Texas A&M University, College Station, Texas, USA.

also occurred in the tropics, but may have started later than at high latitudes [Pearson *et al.*, 2007]. The transition however, was dynamic and punctuated by at least one distinct climate reversal at ~40 Ma, the Middle Eocene Climatic Optimum (MECO) and several upper Eocene calcite accumulation events (CAEs) associated with cooling [Bohaty and Zachos, 2003; Coxall *et al.*, 2005; Lyle *et al.*, 2005; Bohaty *et al.*, 2009]. The MECO was a global event, but it is not clear whether the CAEs occurred outside the equatorial Pacific, and whether these events resulted from increased productivity and/or higher CaCO₃ preservation [Olivarez Lyle and Lyle, 2006].

[4] At the end of the Eocene, around 34 Ma, high latitude surface waters cooled substantially (most evident in the Southern hemisphere), followed by cooling of global deep waters [e.g., Zachos *et al.*, 1996; Thomas *et al.*, 2006; Katz *et al.*, 2008; Lear *et al.*, 2008; Cramer *et al.*, 2009], while Antarctic ice volume increased [Zachos *et al.*, 1992, 1994; Coxall *et al.*, 2005; Miller *et al.*, 2005a, 2005b, 2008; Pälike *et al.*, 2006; Lear *et al.*, 2008]. At northern high latitudes, cooling may have been accompanied by increased seasonality [Eldrett *et al.*, 2009]. Considerably smaller temperature changes may have occurred in surface waters at low latitudes [Wei, 1991; Zachos *et al.*, 1994, 1996; Pearson *et al.*, 2007; Lear *et al.*, 2008; Liu *et al.*, 2009]. Although there is some debate as to whether small polar ice sheets developed earlier in the Eocene [e.g., Miller *et al.*, 2005b; Tripathi and Elderfield, 2005; Edgar *et al.*, 2007; Burgess *et al.*, 2008; Hollis *et al.*, 2009], a scenario including major increase in ice volume and global cooling just after the E/O boundary (at oxygen isotope event Oi-1) is widely accepted [e.g., Berggren and Prothero, 1992; Zachos *et al.*, 1994, 2001; DeConto and Pollard, 2003; Thomas *et al.*, 2006; Edgar *et al.*, 2007; Lear *et al.*, 2008; Liu *et al.*, 2009].

[5] Synchronous with the ice buildup, the CaCO₃ compensation depth (CCD) in the Pacific Ocean deepened dramatically (by ~1200 m) and rapidly (in only 300,000 years) [e.g., Van Andel, 1975; Coxall *et al.*, 2005; Rea and Lyle, 2005; Lyle *et al.*, 2008]. A combination of increased continental weathering, and/or changes in ocean circulation and thus deep water chemistry may have led to the deepening of the lysocline and CCD [e.g., Van Andel, 1975; Zachos *et al.*, 1996; Rea and Lyle, 2005; Scher and Martin, 2006; Miller *et al.*, 2008]. It has been suggested that deep water ventilation and meridional overturning circulation in a “greenhouse world” (e.g., the Eocene) was dramatically different from that in an “icehouse world” (e.g., after the start of the Oligocene). During warm conditions, surface ocean current speeds and tropical cyclone activity may have been higher, resulting in lower vertical density gradients and more vigorous diapycnal mixing [Emanuel, 2002; de Boer *et al.*, 2007; Sriver and Huber, 2007; Cramer *et al.*, 2009]. These different patterns of ocean ventilation may have affected deep water chemistry as well as the intensity of oceanic upwelling and nutrient supply to surface waters [e.g., Sarmiento *et al.*, 2004; Moore *et al.*, 2008] and thus the transfer of organic matter to the seafloor [Thomas, 2007]. Changes in sea level related to glaciation may have also caused changes in loci of ocean productivity and the distribution of carbonate and organic

carbon deposition (shelf-basin fractionation) [Merico *et al.*, 2008]. Primary productivity, ecosystem structure, and ocean circulation jointly determine the CaCO₃: C_{org} export ratio and provide feedbacks to modulate pCO₂ and climate.

[6] If surface ocean circulation patterns (e.g., the strength of upwelling and other circulation patterns impacting nutrient distribution and ecosystem structure) also changed as a result of climate shifts, export production would have been impacted. Indeed, important changes in oceanic ecosystems occurred during the late Eocene through earliest Oligocene [see Berggren and Prothero, 1992; Prothero *et al.*, 2003, and reference therein; Falkowski *et al.*, 2004; Finkel *et al.*, 2005].

[7] Although it has been suggested that CaCO₃: C_{org} decreased at the E/O boundary, possibly causing atmospheric pCO₂ to drop [e.g., Diester-Haass and Zahn, 2001; Pagani *et al.*, 2005; Thomas *et al.*, 2006; Liu *et al.*, 2009], no global record of this ratio has been reconstructed. Moreover, it is not clear whether changes in this ratio during the late Eocene CAEs were similar to changes at the E/O boundary [Lyle *et al.*, 2005]. CaCO₃ accumulation on the seafloor reflects both surface and deep-water processes, but export production of C_{org} responds primarily to surface ocean processes. Accordingly, CaCO₃ accumulation and export production could be decoupled. In addition, export production to the deep-ocean and C_{org} burial in the sediment can also be decoupled due to early diagenetic C_{org} regeneration which further complicates interpretation of records of these processes [Olivarez Lyle and Lyle, 2006; Thomas, 2007].

[8] We record CaCO₃ and barite accumulation rates (CAR and BAR) in two regions of the Pacific Ocean and use these records to reconstruct changes in inorganic C (CaCO₃) burial and export production (C_{org} export) from 40 to 32 Ma, during the transition from a ‘greenhouse’ to ‘icehouse’ climate. Excess Ba data have been previously published for ODP Site 1218 in the equatorial Pacific (ODP Leg 199 [Shipboard Scientific Party, 2002b]). In this study, we separated barite from sediments to reconstruct barite accumulation rates (BAR), thus eliminating some of the potential complications associated with the construction and interpretation of excess Ba as a proxy for export production [Averyt and Paytan, 2004].

[9] Marine barite (BaSO₄) is a common, albeit minor, component of marine sediments, and is especially abundant in sediments underlying areas of high productivity [e.g., Church, 1970]. A strong correlation between BAR and organic C export has been observed in core top sediments [Paytan *et al.*, 1996; Eagle *et al.*, 2003]. Assuming the processes that govern barite formation and preservation remained constant through time, changes in BAR reflect variations in export production. Indeed, BAR and excess Ba have been widely used to reconstruct changes in export production through time [Schmitz, 1987; Rutsch *et al.*, 1995; Paytan *et al.*, 1996; Dean *et al.*, 1997; Nürnberg *et al.*, 1997; Bonn *et al.*, 1998; Bains *et al.*, 2000; Martínez-Ruiz *et al.*, 2003; Averyt and Paytan, 2004; Jaccard *et al.*, 2005; Olivarez Lyle and Lyle, 2006].

[10] Our BAR data are compared to the excess Ba results for Site 1218 and BAR data from other locations in the Pacific (DSDP Site 574 and ODP Sites 1209–1211), in order to

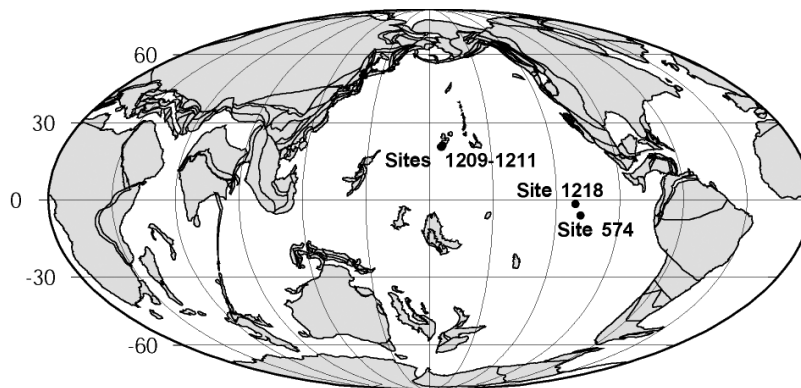


Figure 1. Approximate late Eocene locations of DSDP Site 574 (Leg 85); ODP sites 1209, 1210, and 1211 (Leg 198); and Leg 199 Site 1218 plotted on a paleogeographic reconstruction 40 Ma by the Ocean Drilling Stratigraphic Network (<http://www.geo-guide.de/cgi-bin/ssgfi/anzeige.pl?db=geo&nr=001109&ew=SSGFI>). Plates were moved relative to the ODSN Hot Spot Ref. Frame 1.

obtain a broader geographic representation and better understanding of the processes controlling ocean productivity over this time interval.

2. Methods

2.1. Site Descriptions

[11] Samples were obtained from Ocean Drilling Program Leg 198 Sites 1209, 1210, and 1211 on Shatsky Rise in the Central Basin of the North Pacific Ocean and from Sites 1218 and 574 in the eastern equatorial Pacific (Figure 1). Shatsky Rise is an oceanic plateau at 35°N, 160°E in the Pacific Ocean. Site 1209 is at 2,387 m depth (paleodepths between 40 and 32Ma ~2000 to ~2100 m), Site 1210 at 2,573 m depth (paleo depths ~2200 to ~2300 m), and Site 1211 at 2,907 m depth (paleo depths ~2600 to ~2700 m) [Bohaty *et al.*, 2009]. The shallow water depths and sediment burial depths at this location result in high CaCO₃ content, as estimated by reflectance data (ODP Leg 198 [Shipboard Scientific Party, 2002a]) and measured in this study (Data Set S1).¹ Sediments from Site 1209 show a marked color change, from light brown/tan to gray/white, at the transition from the Eocene into the Oligocene, whereas Sites 1210 and 1211 contain cycles of lighter and darker sediments superimposed on a gradual lightening through time (ODP Leg 198 [Shipboard Scientific Party, 2002a]). Samples were collected from the upper Eocene through the E/O boundary interval with a resolution of one sample every 16 cm to 30 cm, depending on sample availability.

[12] Site 1218 (ODP Leg 199) at 8.5°N 135.2°W, 4,828 m water depth (paleo depths between 40 and 32Ma ~3500 to ~3800 m; Scientific Party ODP Leg 199, 2002) is situated on a basement swell ~3°N of the Clipperton Fracture Zone in the eastern tropical Pacific and remained within 2° of the equator from the time crust was formed until 27 Ma (ODP Leg 199 [Shipboard Scientific Party, 2002b]). The upper Eocene sediments are primarily composed of radiolarites and nan-

nofossil chalk with occasional chert beds (ODP Leg 199 [Shipboard Scientific Party, 2002b]). The E/O boundary is abrupt, with a rapid transition from Eocene dark radiolarites to Oligocene pale nannofossil ooze and chalk. Samples were collected between 220 and 275 m composite depth (mcd), corresponding to 40–32 Ma (Data Set S1). Dry Bulk Density (DBD), mass accumulation rates (MAR), C_{org}, excess Ba, biogenic silica and CaCO₃ content were previously determined [Coxall *et al.*, 2005; Lyle *et al.*, 2005; Olivarez Lyle and Lyle, 2006], and an orbitally tuned chronology based on benthic foraminiferal δ¹⁸O values is available [Pälike *et al.*, 2006]. The increase in CCD at the E/O boundary, as recorded at this site, was fast and occurred in two steps (40 kyr each separated by 200 kyr). Based on δ¹⁸O records [Coxall *et al.*, 2005; Pälike *et al.*, 2006] it has been suggested that deep waters cooled during the transition (but see also Lear *et al.* [2008]). C_{org} preservation in Eocene sediments was low, but excess Ba fluctuations suggest that export productivity fluctuated strongly, with higher export productivity during cooler periods of the Eocene [Olivarez Lyle and Lyle, 2006].

[13] For comparison, samples representing the time interval between 37.5 and 32.5 Ma were obtained from Deep Sea Drilling Project Site 574 in the same region (DSDP Leg 85; 4.12°N 133.2°W; 4,571 m depth; paleo-depths between 37 and 32 Ma of ~3200 to ~3500 m) (Data Set S1). Low recovery (29%; DSDP Leg 85 [Shipboard Scientific Party, 1985]) between 517.5 and 508 m below seafloor (mbsf) precluded the collection of a complete record at this site.

2.2. Carbonate Content Analysis

[14] For Sites 1209–1211, sediment samples were dried and ground to a powder. Three to five mg of crushed homogenized sample was analyzed for carbonate content using a coulometer (UIC Inc. Coulometrics) [Averyt *et al.*, 2005]. The instrumental precision is ~0.8%, and reproducibility (determined by running duplicate samples) is better than 1% (Data Set S1). Sediments from Site 574 were similarly dried and homogenized and carbonate content was measured by coulometry (UIC Inc. CM5012 coulometer and

¹Auxiliary material data sets are available at <ftp://ftp.agu.org/apend/pa/2010pa001932>.

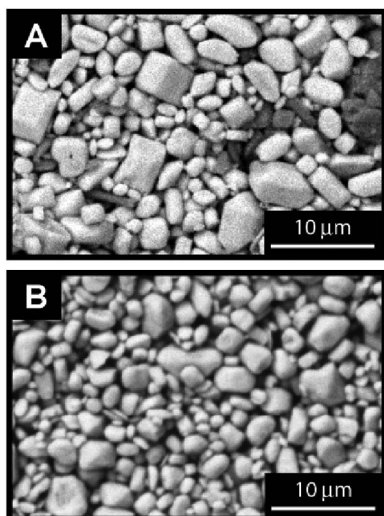


Figure 2. Barite crystals viewed with a Scanning Electron Microscope: (a) ODP Site 1209C 4-2, ca. 33 Ma and (b) ODP Site 1218A 24-6, ca. 35 Ma.

CM 5120 combustion furnace) at Texas A&M University as described by Lyle *et al.* [2005].

[15] Carbonate content data for Site 1218 were obtained from Lyle *et al.* [2005] for samples > 34Ma. For Site 1218 samples < 34Ma, ODP shipboard measurements of wt % Ca [Shipboard Scientific Party, 2002b] were converted to wt % CaCO₃ using equation (3) of Dymond *et al.* [1976] to correct total Ca in sediments for sea salt and other non-carbonate contributions.

2.3. Sand Fraction Analysis

[16] We used the weight percent of the sand fraction as a measure of CaCO₃ preservation in high CaCO₃ sediments [e.g., Frenz *et al.*, 2006]. Samples were dried and weighed and wet-sieved through a 63 μm screen. If further disaggregation was needed, samples were exposed to 10% H₂O₂ and ultrasound for 2 min before repeat sieving (Data Set S2).

2.4. Barite Separation

[17] Ten to thirty grams of dry sediment was used for barite separation, depending on the amount of sample available. A sequential leaching procedure was used to remove all sedimentary components except barite and a small amount of other resistant materials [Eagle *et al.*, 2003]. Barite recovery (yield) in this process is better than 90% [Eagle *et al.*, 2003; Gonnee and Paytan, 2006]. Sample residues for this study typically contained more than 90% barite, with all but three samples above 80% barite. A SEM photo of a typical sample residue with barite crystals is shown in Figure 2.

2.5. Age Models

[18] The age model for Site 1218 is the most reliable and has the highest time resolution; we used the published age model for this site [Coxall *et al.*, 2005; Pälike *et al.*, 2006]. We used the biostratigraphic datum levels in the work by Barron *et al.* [1985] for DSDP Leg 85 Site 574 and the oxygen isotope data in the work by Miller and Thomas

[1985], adapted to the numerical ages in the work by Pälike *et al.* [2006]. This age model has changed slightly from that used by Ravizza and Peucker-Ehrenbrink [2003], based on the same datum levels with numerical ages as in the work by Berggren *et al.* [1995]. There are, however, no reliable datum levels below the Eocene/Oligocene boundary at this site, and the age model is therefore not well constrained for the Eocene part of the record. The accumulation rates of Oligocene sediment at Site 574 are similar to those at Site 1218, and therefore we constructed the age model for the Eocene part of Site 574 using the same ratio of accumulation between the sites for the Eocene as during the Oligocene.

[19] Available late Eocene to early Oligocene age models for the sites drilled on ODP Leg 198 (Sites 1208, 1209, 1210), also based on the work by Berggren *et al.* [1995] are much less highly resolved. There are apparent disparities between the datum levels of planktonic foraminifera [Petruzzo *et al.*, 2005] and calcareous nannofossils [Bralower, 2005]. These disparities may result from true differences in the relative sequence of planktonic foraminifera and nannofossil events in the Pacific and the sites where the Berggren *et al.* [1995] time scale was calibrated.

[20] We compiled the biostratigraphic datum levels (Table 1), assigned numerical ages as in the work by Pälike *et al.* [2006], and used age-depth plots to evaluate which datum levels appeared to present the most consistent pattern. Using these datum levels resulted in age models which generally gave temporally consistent trends in BAR and CAR across all sites. We accepted this age model tentatively because BAR in oxic sediments is representative of processes in the upper water column (e.g., export production), and one would expect that broad changes in export productivity (as recorded by BAR) would occur about simultaneously at all three sites which are in close proximity (approximately 50 km apart; ODP Leg 198 [Shipboard Scientific Party, 2002a]). However, the magnitude of the BAR changes is expected to differ among sites as a result of the depth dependence of barite preservation [e.g., Paytan and Griffith, 2007]. The similarity of timing and trends in magnitude do not necessarily apply to CAR [see Zachos *et al.*, 2005].

Table 1. Datum and Ages Used for Age Model Reconstruction for Leg 198 Sites

Event	Age (Ma)	Depth (mcd)	Source
<i>Leg 198, Site 1209</i>			
FO <i>Sphenolithus distentus</i>	30.32	129.66	Bralower [2005]
LAD <i>Hantkenina</i>	33.70	137.11	Petruzzo <i>et al.</i> [2005]
LAD <i>C. grandis</i> (37.1 Ma)	37.10	137.73	Bralower [2005]
LAD <i>N. fulgens</i>	43.40	151.11	Bralower [2005]
<i>Leg 198, Site 1210</i>			
LAD <i>E. formosa</i>	32.90	130.77	Bralower [2005]
LAD <i>D. barbadiensis</i>	34.20	136.68	Bralower [2005]
LAD <i>C. grandis</i> (37.1 Ma)	37.10	137.59	Bralower [2005]
LAD <i>N. fulgens</i>	43.40	152.41	Bralower [2005]
<i>Leg 198, Site 1211</i>			
LAD <i>E. formosa</i>	32.90	80.20	Bralower [2005]
LAD <i>Hantkenina</i>	33.70	82.83	Petruzzo <i>et al.</i> [2005]
LAD <i>D. barbadiensis</i>	34.20	86.90	Bralower [2005]
FO <i>Ismolithus recurvus</i>	36.60	89.55	Bralower [2005]
LAD <i>N. fulgens</i>	43.40	98.75	Bralower [2005]

2.6. Mass Accumulation Rates

[21] Bulk sediment mass accumulation rates ($\text{g cm}^{-2} \text{kyr}^{-1}$) for Leg 198 and Site 574 samples were calculated from the dry bulk density (g cm^{-3}) of the sample and sedimentation rate (cm kyr^{-1} see above). Dry bulk density was calculated from the percent CaCO_3 of each sample [Snoeckx and Rea, 1994] or taken from the respective shipboard data. For Site 1218, mass accumulation rates are extrapolated from values in the work by Lyle *et al.* [2005]. The barite accumulation rate (BAR) and CaCO_3 accumulation rate (CAR) were calculated from the bulk mass accumulation rate (MAR) for each sample and the wt % barite and wt % CaCO_3 in the sample, respectively (Data Set S1). The largest errors in the proxy data presented here (BAR and CAR) stem from errors associated with MAR determination. These errors are predominantly driven by uncertainty in age models that impact sedimentation rate calculations and thus MAR. As indicated above, age models are least constrained for Leg 198 sites. However, changes in age model of ± 0.25 Ma do not change the general trends observed in the proxy data and thus will not impact the major conclusions from these data.

3. Results

[22] Wt % CaCO_3 , barite, and coarse fraction were plotted versus depth for each site (Figure 3). The shallower North Pacific sites (Leg 198) are generally characterized by high wt % CaCO_3 (>90%). At the deeper equatorial Pacific Sites 1218 and 574, wt % CaCO_3 is typically low (<70%), with fluctuations between 0 and 70% in the upper Eocene, and a pronounced increase in wt % CaCO_3 to 85–90% at the E/O boundary. Barite wt % in the North Pacific (Leg 198) sites is typically low, ranging from zero to approximately 0.5%. Barite content decreases by about a factor of two up core from 139 mcd at Sites 1209 and 1210, and from 88 mcd at Site 1211. The wt % barite decreases with water depth. The percent coarse fraction at these sites increases at about the same levels in the cores where the barite wt % decreases. The wt % barite at the equatorial Pacific (Sites 1218 and 574) is much higher (ranging between 0.2 and 1.5%) than at the North Pacific sites. The wt % barite at these cores decreases about 10-fold up core at 240 and 502 mbsf, respectively, where CaCO_3 increases.

[23] The wt % CaCO_3 is significantly negatively correlated with the wt % barite at all sites (Figure 4), suggesting that barite content is in part determined by dilution by CaCO_3 , highlighting the need to use MARs [Dymond *et al.*, 1992; Paytan *et al.*, 1996; Eagle *et al.*, 2003; Averyt and Paytan, 2004]. The imperfect linearity between wt% CaCO_3 and wt % barite indicates that dilution is not the only control on wt% barite and that changes in barite content and accumulation were driven by other factors. The CaCO_3 accumulation rate (CAR) and barite accumulation rate (BAR) versus age for each site are shown in Figure 5 and CAR:BAR ratios are shown in Figure 6.

[24] At the Leg 198 North Pacific (Shatsky Rise) sites, at paleolatitudes of ca. 15°N, both BAR and CAR were relatively high before about 37.5 Ma, then decreased and remained low until just below the E/O boundary (at 33.7 Ma), at which time both BAR and CAR increased at all 3 sites.

CAR values were higher after the E/O boundary (typically > $0.4 \text{ g cm}^{-2} \text{ kyr}^{-1}$) than before 37.5 Ma ($\sim 0.25 \text{ g cm}^{-2} \text{ kyr}^{-1}$). There are no clear CAEs at these sites in the upper Eocene, whereas distinct BAR peaks are evident. BAR values above the E/O boundary are also higher ($\sim 0.1 \text{ mg cm}^{-2} \text{ kyr}^{-1}$) than below it (between 37.5 and 33.5 Ma), but not as high as values typical for the period before 37.5 Ma (up to $0.8 \text{ mg cm}^{-2} \text{ kyr}^{-1}$ at Site 1209). The magnitude of change in CAR during the E/O transition is much larger than the magnitude of change in BAR. At our sampling resolution, the changes in CAR and BAR occurred nearly simultaneously at these three sites.

[25] At the equatorial Pacific sites, CAR varied from about 0.01 to over $2 \text{ g cm}^{-2} \text{ kyr}^{-1}$; with maxima at ~ 39 Ma (CAE-4) and ~ 36 Ma (CAE-6) [Olivarez Lyle and Lyle, 2006]. A pronounced increase in CAR occurs at the E/O boundary (from ~ 0.02 to over $1.0 \text{ g cm}^{-2} \text{ kyr}^{-1}$). These CAR are generally higher at the equatorial Pacific sites than at the North Pacific sites as expected from their location within the Pacific high productivity region. BAR values were also much higher in the equatorial region than at the North Pacific sites (ranging from 0.5 to $\sim 8 \text{ mg cm}^{-2} \text{ kyr}^{-1}$), with distinct fluctuations and peaks corresponding to the CAR peaks at ~ 39 Ma ($4 \text{ mg cm}^{-2} \text{ kyr}^{-1}$) and ~ 36 Ma ($8 \text{ mg cm}^{-2} \text{ kyr}^{-1}$). The magnitude of the CAR peaks decreased from CAE-4 to CAE-6, but the intensity of the BAR peaks remained constant or even increased. The peaks in CAR and BAR at Site 1218 correspond to small increases in the $\delta^{18}\text{O}$ record [Lyle *et al.*, 2005], suggesting that high CAR and BAR may be associated with cooling events. Smaller but distinct increases in BAR occurred also during the E/O transition at 34.2 Ma and 33.7 Ma (Figure 5). Our BAR data for Site 1218 generally agree well with excess Ba data presented by Olivarez Lyle and Lyle [2006], indicating that much (but not all) of the excess Ba at this site is associated with barite (Figure 7). Relative trends in CAR and BAR at Site 574, where available, agree with those from Site 1218 although absolute accumulation rates are slightly higher (Figure 5).

[26] We used an empirical core top correlation between BAR and export production [Eagle *et al.*, 2003; Paytan *et al.*, 1996] based on equatorial Pacific cores from the same depth range to calculate C export ($\text{g C m}^{-2} \text{ yr}^{-1}$) for various time slices (Table 2). In the equatorial Pacific, C export was about a factor of 3–4 higher during the late Eocene CAEs than during non-CAE periods (~ 20 versus ~ 60 – $80 \text{ g C m}^{-2} \text{ yr}^{-1}$). During the glacial event at the Eocene-Oligocene boundary (Oi-1), C export increased by a factor of 2 from ~ 20 to $40 \text{ g C m}^{-2} \text{ yr}^{-1}$ at the equator. These values generally agree with new productivity (C_{org} export) values derived from estimates by Olivarez Lyle and Lyle [2006] of C rain to the sediment, as calculated from measured excess Ba (Bio-Barium) for Site 1218, using the predictive equation from Sarnthein *et al.* [1988] following Dymond *et al.* [1992] (Table 2). Export production at Site 574, located south of the equator during this time interval, was generally higher than at the equatorial Site 1218.

[27] It should be noted that the absolute value of calculated C export flux (export production) depend on the assumption that (1) the same processes governing barite production and preservation in the ocean today have operated in the past and (2) the calibration between BAR and export production based

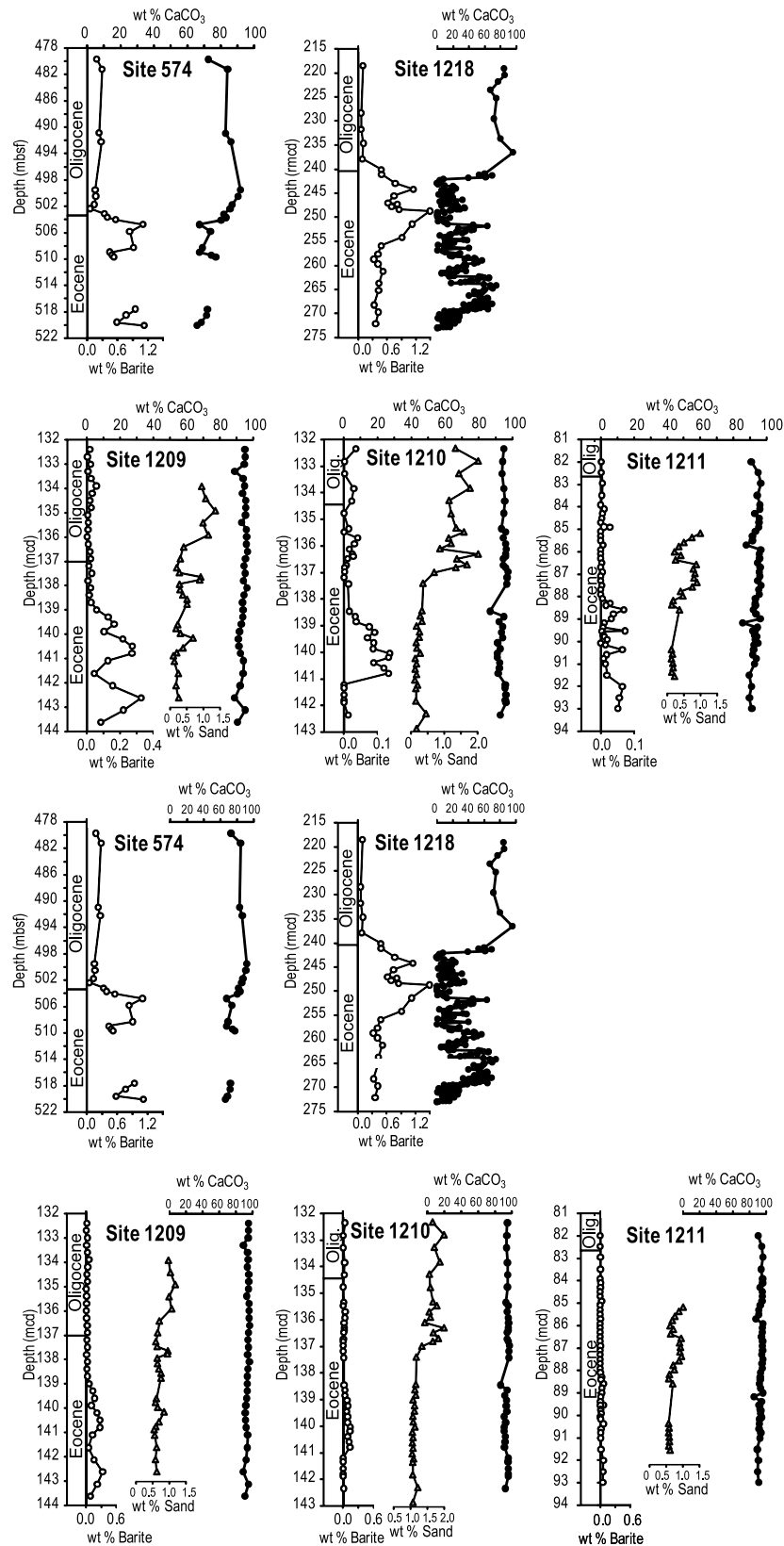


Figure 3. Weight percent (wt %) barite (open circles), CaCO₃ (solid circles), and sand fraction (triangles) plotted with depth in core. The plot is shown both on the same scale for all sites and using different scales for each site to compare among sites and to reflect differences in measured values within each site respectively.

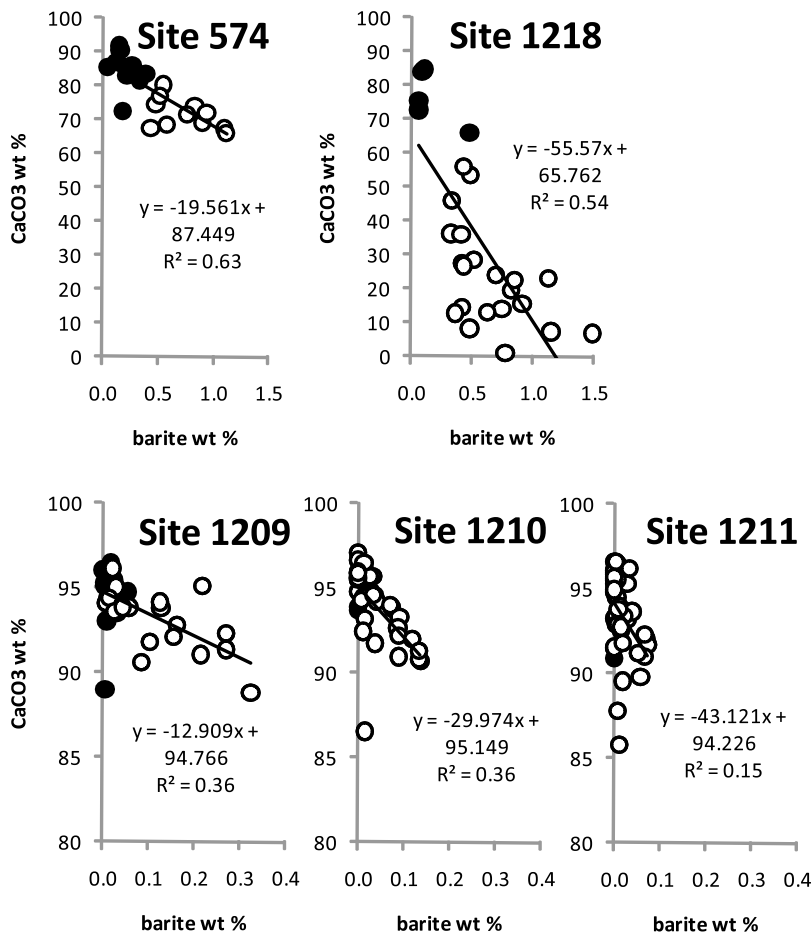


Figure 4. Barite wt % versus CaCO_3 wt %. Note different scales are used for each region to reflect differences in measured values. Open symbols are for Eocene samples and solid symbols are for Oligocene samples. The non perfect linearity indicates that BAR is not controlled only by dilution with CaCO_3 .

on present-day core top data is valid for other times. While this assumption cannot be verified, the values obtained seem reasonable and the trends are consistent with current understanding of ocean processes lending support to the calculated values and their interpretation.

4. Discussion

[28] CaCO_3 content and accumulation in open-ocean marine sediments is controlled primarily by CaCO_3 productivity (rain flux of calcifying organisms) and preservation at the seafloor. Changes in the abundance of calcifiers due to changes in nutrient availability or surface temperature and pH as well as changes in carbonate saturation of intermediate and deep waters (due to changes in temperature and carbonate chemistry) will result in fluctuations in CaCO_3 content in the sediment [e.g., Van Andel, 1975; Theyer *et al.*, 1985; Lyle *et al.*, 2008]. Barite accumulation in oxic sediments responds primarily to export production, although a smaller effect of depth-dependent preservation has also been recognized [Paytan and Griffith, 2007]. Comparing the records of CAR and BAR through time and in space may shed light on the co-variation or decoupling of export productivity and

CaCO_3 preservation and their relation to oceanic and climatic changes. In addition, comparison of BAR derived export production to other paleo-productivity proxies such as biogenic silica and authigenic phosphorus accumulation may elucidate the controls and sensitivity of each of these proxies.

4.1. Carbonate and Barite Abundance and Accumulation in the Late Eocene

[29] Strong fluctuations in wt % CaCO_3 and CAR occurred at the deep equatorial Pacific sites during the late Eocene. Two distinct maxima corresponding to CAE-4 at ~39 Ma and CAE-6 at ~36 Ma, and two smaller maxima corresponding to CAE-5 and CAE-7 are evident [Lyle *et al.*, 2005]. CAEs have been described as weaker analogs of the extreme cooling Oi-1 event just after the E/O transition [Coxall *et al.*, 2005; Lyle *et al.*, 2005]. These authors speculated that the association of high CaCO_3 and cooling during these events have resulted from decreased CaCO_3 dissolution at the sediment water interface, following changes in ocean circulation bringing colder (“younger”) waters with higher pH and carbonate ion concentrations to the equatorial Pacific. However, these peaks may alternatively be explained as increases in carbonate productivity resulting from higher nutrient availability

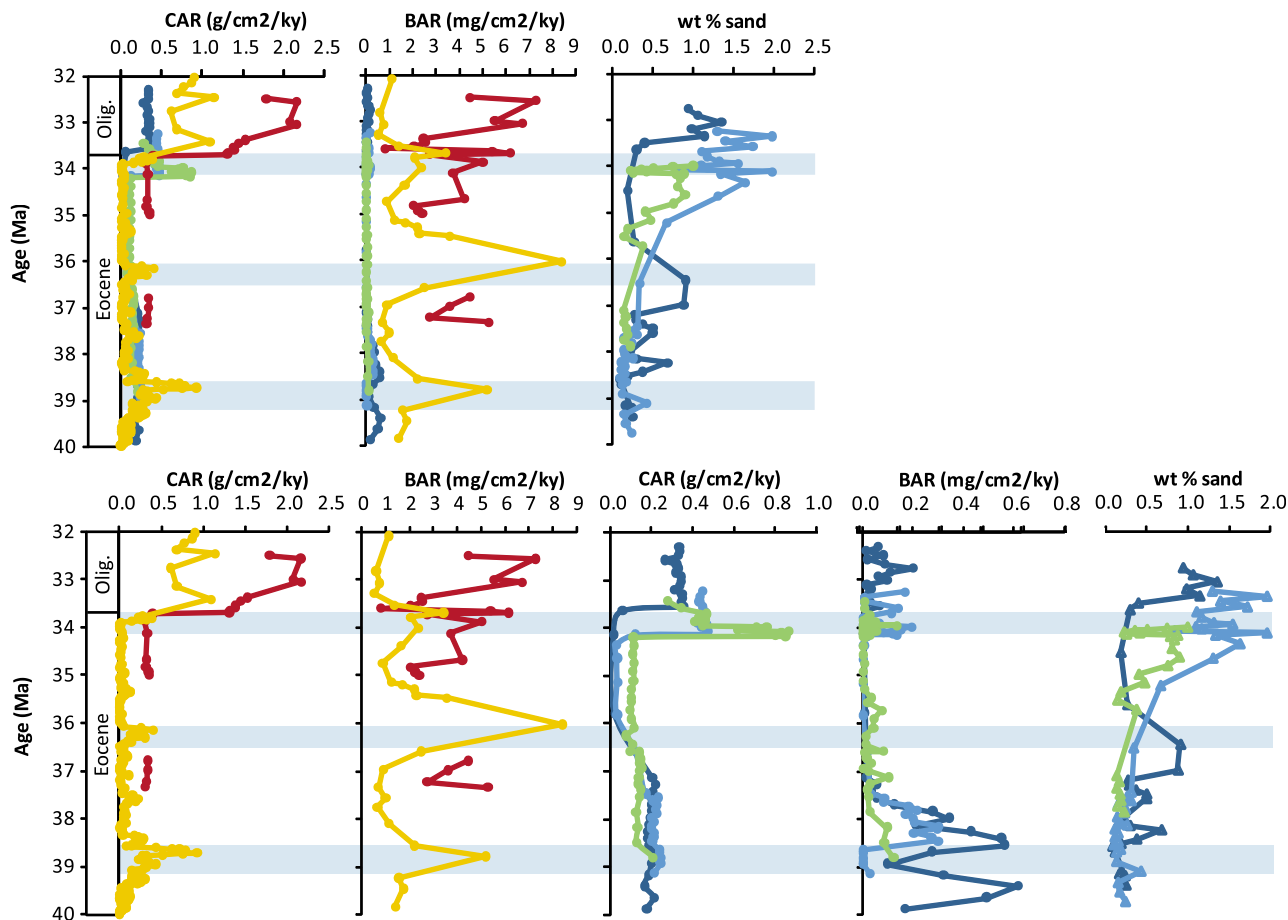


Figure 5. Barite accumulation rate (BAR), carbonate accumulation rate (CAR), and sand fraction plotted versus age (million years ago, Ma). Data shown on the same scale for comparison among sites and on different scales to reflect differences in calculated values within each core. Site 574 is red, Site 1218 is yellow, Site 1209 is dark blue, Site 1210 is light blue, and Site 1211 is green. Shaded areas represent CAE-4, CAE-6, and Oi-1 (from oldest to youngest).

or a combination of both increased productivity and preservation. Indeed, all CAE peaks seen in the equatorial Pacific (Site 1218) are associated with increased export production, as seen from increased BAR. The amplitude of the various CAEs for CAR and BAR does not vary similarly; while maximum CAR decreases from CAE-4 to CAE-6, peak BAR remained constant or slightly increased from CAE-4 to CAE-6. The decrease in the magnitude of the CAR maxima from CAE-4 to CAE-6 resulted primarily from lower wt % CaCO_3 , although bulk MAR also decreased slightly [Lyle *et al.*, 2005].

[30] If CaCO_3 productivity is proportional to total export productivity, one would expect similar trends in CAR and BAR maxima. Decoupling in magnitude indicates that CAR during the CAEs is controlled both by an increase in carbonate productivity and by changes in its preservation. This would imply a decrease in carbonate preservation and increase in water masses corrosiveness toward the Oligocene during these repetitive cooling events. Such a trend indicates that the characteristics of the source of dense bottom water changed over time (becoming more corrosive), and/or that the

relative contribution of a “younger” i.e., less corrosive colder water masses to the equatorial Pacific progressively decreased during each of the CAEs (toward the Oligocene).

[31] The correspondence between cooling events during CAEs and export productivity suggests that changes in the efficiency of the biological pump were forced by the climatically mediated changes which impacted ocean circulation. Similar productivity peaks of smaller magnitude with the same correspondence to temperature are also seen in the Southern Ocean [Diester-Haass and Zahn, 2001]. Anderson and Delaney [2005] also describe several peaks in productivity indicators (Ba, opal and P) during the same time interval in the South Atlantic and Southern Ocean. Increased wind stress and Ekman transport and upwelling of nutrient rich subsurface water was postulated as a cause of these productivity oscillations [Diester-Haass and Zahn, 2001; Huber and Caballero, 2003; Wunsch and Ferrari, 2004]. While it is not clear that the productivity peaks throughout the world’s oceans were synchronous it is evident that the mid to late Eocene was characterized by repeated cycles of highs and lows in ocean productivity. We note that BAR represents

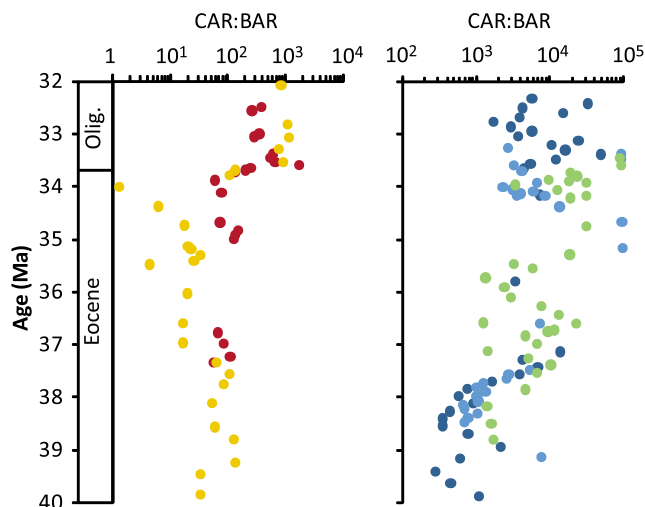


Figure 6. CAR:BAR ratios versus age (Ma). Samples with BAR = 0 were not included. Site 574 is red, Site 1218 is yellow, Site 1209 is dark blue, Site 1210 is light blue, and Site 1211 is green.

export production and it is possible that primary production during these cold events did not change much but the efficiency of the biological pump may have been higher, resulting in higher export. For example, cooler, high-nutrient water may have favored diatom productivity over that by other phytoplankton resulting in increased export of C_{org} to depth [Falkowski *et al.*, 2004]. Indeed biogenic silica accumulation rates in the equatorial Pacific and in the Southern Ocean were higher during the CAEs [Anderson and Delaney, 2005; Lyle *et al.*, 2005; Olivarez Lyle and Lyle, 2006]. Specifically, at Site 1218 in the mid Eocene where both BAR (this work) and biogenic silica [Olivarez Lyle and Lyle, 2006] were determined on the same core (although not the same samples) they correspond well (see Figure S1). If CO_2 fixation by phytoplankton surpassed CO_2 fluxes out of the ocean in the equatorial upwelling and other regions during the cooling events, this may have provided a positive feedback, further drawing down atmospheric CO_2 and intensifying the cooling trend.

[32] At the North Pacific sites (Leg 198) wt % $CaCO_3$ is much higher than in the equatorial Pacific throughout the record (although MARs are generally lower). These sites were above the CCD throughout the sampled interval, thus the $CaCO_3$ content is so high (90–96%) that fluctuations in wt % $CaCO_3$ are not easily resolved. There is no clear indication of the late Eocene CAEs. The percent coarse fraction is an alternative measure of $CaCO_3$ preservation, but no systematic change in percent coarse fraction occurred during equatorial Pacific CAEs. This suggests that strong fluctuations in CAR during the late Eocene were restricted to the equatorial area or occurred below paleo-depths of ~ 3 km. Indeed, the lower CAR at Site 1218 compared to Site 574 may be due to difference in paleo-depth (~ 3700 m and ~ 3200 m, respectively) consistent with a depth dependent preservation effect of $CaCO_3$ below 3 km depth.

[33] In contrast to the CAR, small but distinct upper Eocene BAR peaks are observed at the Shatsky Rise sites, which are offset in timing from the equatorial CAEs. The age models for the Shatsky Rise and therefore estimates of accumulation rates are based on limited biomarker data because of poor preservation (Table 1) thus the apparent offsets may well stem from inadequacies of our age models. A similar trend of peak accumulation in Ba, P and opal in Southern Ocean sites which is not accompanied by high carbonate accumulation [Anderson and Delaney, 2005] may suggest that the productivity peaks are indeed a temporally consistent and global feature. We can, however, not exclude the possibility that fluctuations in the export flux were diachronous in different regions of the Pacific. Many parameters controlling primary and export production tend to be regional. During the late Eocene, Shatsky Rise was within the southern edge of the N. Pacific gyre and may have not been affected by the equatorial high productivity events. The fluctuations in export production at these northern sites (like in the Southern Ocean) are not accompanied by a change in $CaCO_3$ preservation, as in the equatorial sites, suggesting that $CaCO_3$ productivity did not change linearly with export production, or that $CaCO_3$ productivity was only a small component of the total production.

[34] The fluctuations in BAR at all three Shatsky Rise sites are, despite the uncertainties in the age models, consistent in timing but not in magnitude with BAR decreasing with depth. The decreasing BAR trend with increasing water depth is also

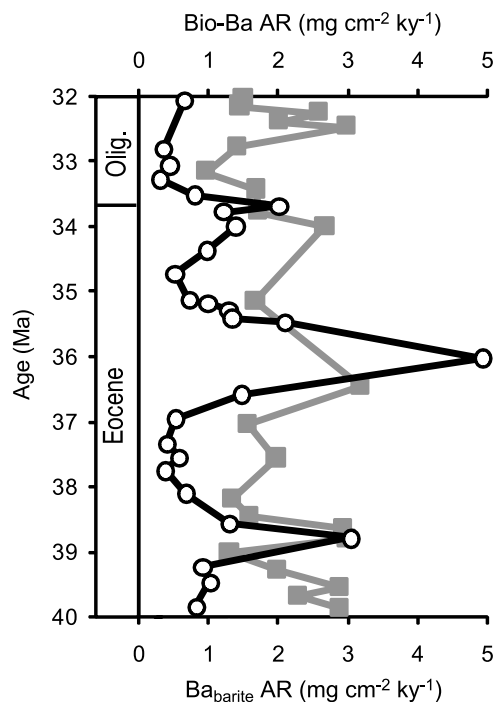


Figure 7. Site 1218 Ba accumulation rate (Ba_{barite} AR) calculated from barite wt % (this study; black open circles) and excess Ba or Bio-Ba [Olivarez Lyle and Lyle, 2006] (gray solid squares) versus age (million years ago, Ma).

Table 2. Export Production Calculations Based on Barite Accumulation Rates Or Excess Ba From *Olivarez Lyle and Lyle* [2006] for Different Age Slices Between 40 and 32 Ma^a

	Age (Ma)	Lat	Long	Water Depth (m)	Pnew From Bio-Ba (gC m ⁻² y ⁻¹)	Export Production (gC m ⁻² y ⁻¹)	Bulk MAR (g cm ⁻² ky ⁻¹)	BAR (mg cm ⁻² ky ⁻¹)
JGOFS TT013-69MC ^b	0	0.1N	139.72W	4301	29	50	1.52	2.3
Leg 85, Site 574	Oi-1 (34–33.7)			~3500	ND	max. 69	1.57	3.6
Leg 199, Site 1218	Oi-1 (34–33.7)			~3800	max. 52 ^c	max. 43	0.71	2.0
	CAE 6 (36.5–36)			~3700	max. 64 ^c	max. 89	0.75	4.9
	CAE 4 (39–38.5)			~3500	max. 48 ^c	max. 59	1.22	3.0
	base (40–32)	0 ± 0.4N	106–108W	~3500–3800	~8–16 ^c	~16–24	~0.2–1.5	~0.3–0.8

^aValues based on barite accumulation rates are from this study. ND = not determined. Cores are in the equatorial Pacific.

^bFrom *Eagle et al.* [2003].

^cCalculated from data of *Olivarez Lyle and Lyle* [2006].

observed in the wt % barite data. This trend cannot be the result of decreasing particulate matter concentration with depth in the water column at the paleo-depths of our sites [e.g., *Martin et al.*, 1987]. The difference in particulate organic C (POC) rain rate between 2,000 and 3,000 m is very small because most of the mineralization in the water column occurs at depths shallower than 1,500 m [*Berelson*, 2001]. The sedimentation rates are similar for all three sites, thus changes in sedimentation rates or focusing of sediments can be ruled out as well. We argue that this depth-dependent barite preservation is not directly related to C export or mineralization. Previous studies have shown that the water column becomes less saturated with respect to barite with increasing depths [*Monnin et al.*, 1999; *Rushdi et al.*, 2000; *Monnin and Cividini*, 2006]. Specifically, in the Pacific dissolved Ba profiles result in a pronounced decrease in barite saturation index with depth [*Monnin et al.*, 1999; *Rushdi et al.*, 2000; *Monnin and Cividini*, 2006]. This depth dependent preservation of barite may hinder our ability to compare BAR among sites of different depths although data (A. Paytan, unpublished data, 2007) suggest that the preservation effect is much smaller than that related to productivity. Indeed differences of about twofold are seen in BAR between the various Leg 198 sites compared to an order of magnitude difference between the equatorial and North Pacific sites controlled by absolute differences in export production rates. Regardless, the impact of depth/saturation dependent barite preservation should be further investigated and quantified to improve the use of BARs for export production estimates.

[35] At ~36.5 Ma, both CAR and BAR at the Shatsky Rise sites dropped to very low values and remained low until the E/O boundary. The low values of CAR and high wt % CaCO₃, and their association with low BAR suggest overall low export productivity, not a decrease in preservation. Low MARs just before the E/O boundary (at ~35 Ma) are also observed at the equatorial sites, implying a Pacific-wide trend toward low ocean export production. An uppermost Eocene change from radiolarian ooze to radiolarian clay (fewer fossils) and decreases in the latitudinal width of the zone of biogenic deposition is consistent with this interpretation [*Moore et al.*, 2004]. The wt % sand at the Shatsky Rise sites was higher during the low MAR period (increasing gradually from 36.5 Ma to the E/O boundary), consistent with a decrease in export production, not preservation. This period

of low export production may be related to warming before Oi-1 [*Bohaty and Zachos*, 2003; *Poag et al.*, 2003]. The global nature of this low export production period should be further investigated.

[36] To summarize, the late Eocene is characterized by several long periods of highs and lows in productivity which are observed at multiple locations in the ocean. The correspondence of lower export production with warmer and higher export production with cooler temperatures is likely related to changes in the source (location or depth) and intensity of the upwelling water masses, which likely co-vary with climatically induced deep water circulation changes. In addition, the changes in CAR (at deep sites) in the late Eocene reflect primarily changes in ocean production and to a lesser extent preservation.

4.2. Carbonate and Barite Abundance and Accumulation During the E/O Transition

[37] Wt % CaCO₃ and CAR increased rapidly during the E/O transition at all Pacific sites. The change in CAR at the northern sites indicate that even at these relatively shallow depths, above the CCD, CaCO₃ preservation increased markedly (based on an increase in the coarse fraction and CAR). This is consistent with the well documented deepening of the CCD (and lysocline) at this time in the Pacific [e.g., *Van Andel*, 1975; *Lyle et al.*, 2008] and supports the conclusion that the E/O transition was associated with a global decrease in the “corrosiveness” of deep water masses [e.g., *Diester-Haass and Zahn*, 2001].

[38] CAR at Shatsky Rise increased more at the deepest Site 1211 (paleodepth 2600–2700 m; ~900 mg cm⁻² kyr⁻¹) than at the shallower Sites 1210 (paleodepth 2200–2300m; ~500 mg cm⁻² kyr⁻¹) and 1209 (paleodepth 2000–2100 m; ~350 mg cm⁻² kyr⁻¹). This trend is caused by differences in sedimentation rates among the sites, not by differences in wt % CaCO₃. The relative increase in CAR at the E/O boundary is consistent with deepening of the CCD resulting in a larger net change at the deepest site, but absolute CAR is also higher in the deepest site. CAR is expected to decrease with depth due to increasingly lower saturation state, or to remain constant if all sites were permanently above the lysocline. The period immediately following the E/O boundary thus shows an unusual pattern of CaCO₃ sedimentation, with higher CAR at the deepest site. One potential explanation for the lower

accumulation rates at the shallower sites is higher dissolution rates resulting from higher organic matter oxidation at the sediment water interface and thus lower pore water pH at the time of deposition [Archer, 1996]. However, the observation that the sand fraction is higher at the shallowest site is not consistent with this interpretation, and winnowing of the fine fraction by currents at the shallow site (on a ridge) is more likely. Indeed, it has been argued that bottom currents were more intense just after the E/O boundary as a result of changes in meridional overturning circulation [Scholl *et al.*, 2003].

[39] Following the deepening of the CCD at the E/O boundary, CAR at the equatorial sites was higher than that at Shatsky Rise, despite the greater water depth. This is expected from the location of these sites relative to the highly productive equatorial upwelling belt [Ewing *et al.*, 1968]. The higher equatorial Pacific CAR relative to the North Pacific is also observed at all CAE peaks (Figure 5) despite the lower wt % CaCO₃ in the equatorial Pacific sediments, emphasizing the effect of productivity on CaCO₃ accumulation during CAEs. BAR also increased following the E/O boundary in both regions, but these increases are relatively small compared to the large changes during the CAEs.

[40] The dramatic increase in CAR at the E/O boundary in both regions (and small increase in BAR) combined with the lack of pronounced change during the CAEs at the North Pacific sites may imply different causal mechanisms for these events. Specifically, the CAEs might primarily represent periods of higher productivity and rain rate in the equatorial Pacific. In contrast, during the E/O transition, changes occurred in both regions and carbonate preservation increased pronouncedly, while there is only a small BAR response. The increased productivity during the CAEs if global would be expected to be accompanied by an increase in $\delta^{13}\text{C}$; however, if circulation also changed along with productivity the change might not be apparent at all sites. A similar increase in $\delta^{13}\text{C}$ may be observed also during the E/O, however, these higher values are likely due to changes in circulation and the characteristics of a “younger” less corrosive water mass. In that case a spatial gradient of decreasing $\delta^{13}\text{C}$ might be expected as the water mass moves away from its source region (e.g., if the water source is the Southern Ocean then the North Pacific $\delta^{13}\text{C}$ is expected to be lower than the equatorial sites). These expected trends are consistent with available $\delta^{13}\text{C}$ records [Coxall *et al.*, 2005; Edgar *et al.*, 2007] although more data is needed to verify the spatial trends in $\delta^{13}\text{C}$. We thus argue that the late Eocene fluctuations reflect primarily regional changes in export production related to the source of upwelling water or its intensity, whereas the global and persistent change in CAR across the E/O boundary reflects a pronounced global reorganization of deep sea circulation and seawater chemistry that resulted in a much deeper CCD. It would be, however, desirable to test this hypothesis during a much larger CAE such as CAE-3 to confirm this relationship.

4.3. Trends in Export Productivity in the Pacific Basin

[41] During the late Eocene and early Oligocene, BARs were almost an order of magnitude lower at the Shatsky Rise than in the equatorial Pacific (typically ~ 0.2 and ~ 2 mg cm⁻²

kyr⁻¹, respectively), consistent with present trends in BAR and associated export production (lower in the north by about a factor of 3). This is in agreement with circulation models [Huber and Caballero, 2003] suggesting that in the broadest sense the most basic ocean circulation configuration (upwelling zones and gyres) has not changed much since the late Eocene. Changes in the width (north and south of the equator) and east-west gradients in accumulation as well as smaller features (e.g., off-equator zones of high accumulation) within the broadly defined equatorial high accumulation tongue could have occurred [Moore *et al.*, 2004].

[42] The range of BAR in the equatorial Pacific and calculated export production based on these accumulation rates are similar to those in the Holocene [Paytan *et al.*, 1996; Eagle *et al.*, 2003] (Table 2) and values for Site 1218 are consistent with those calculated by Lyle *et al.* [2008] when converted to export production. The most complete records in both basins (Sites 1209 and 1218), show that, on average, export productivity was higher in the late Eocene than in the very early Oligocene (Table 2). Nevertheless, a peak in BAR is associated with the E-O boundary.

[43] There are several potential reasons for the observed change in export production in these two regions. It is possible that during the warmer parts of the Eocene diapycnal mixing was more vigorous than in the Oligocene increasing productivity [Emanuel, 2002; Anderson and Delaney, 2005; de Boer *et al.*, 2007]. Changes in species composition may also have contributed to the differences in export production [e.g., Falkowski *et al.*, 2004]. Alternatively, the large increase in productivity at high and mid southern latitudes during the E/O transition [Miller *et al.*, 1987; Diester-Haass, 1995, 1996; Diester-Haass and Zahn, 1996, 2001] may have depleted nutrients in the early Oligocene counterpart of Subantarctic Mode Water [Sarmiento *et al.*, 2004], diminishing the nutrient supply to the equatorial and North Pacific regions. The BAR and thus export production apparently were higher at Site 574 ($\sim 4^\circ\text{S}$ at the time) than in the equatorial (Site 1218) and North Pacific sites consistent with nutrient depletion from south to north. It is also possible that the main source of upwelling water in the Eocene was different (and richer in nutrients) than that in the Oligocene, e.g., a North Pacific Intermediate Water source [Sarmiento *et al.*, 2004] or that production was more focused at the equator.

[44] Interestingly, the change in export production at the E/O boundary was much smaller than during the transient late Eocene cooling events (e.g., C export at the CAEs was 1.5–2 times that at the E/O; Table 2). A re-distribution of nutrient resources and loci of high productivity from the equator to high southern latitudes may explain the lower average export production in the equatorial and North Pacific in the Oligocene [e.g., Schumacher and Lazarus, 2004]. It has been suggested that major changes in temperature and ocean circulation at southern high latitudes versus minor changes in the lower latitudes were probably responsible for the geographically disparate changes in productivity fluctuations [Schumacher and Lazarus, 2004]. We emphasize that export production is not always proportional to primary production, and that it is possible that primary production did not change much or could have even increased in the Oligocene relative

to the Eocene, because we cannot exclude that changes in efficiency of the biological pump could have been responsible for the change in export flux to depth.

4.4. Trends in CAR:BAR Ratios

[45] Ratios of CAR:BAR can be used as a proxy for CaCO₃ to C_{org} rain ratios (with the caveat of carbonate dissolution at depth changing the original ratio, thus CAR:BAR may better reflect the CaCO₃ burial to C_{org} rain ratio). Throughout the late Eocene and early Oligocene, the CAR:BAR ratio was higher in the North Pacific gyre than at the equatorial sites, as expected when comparing the low productivity shallow sites to deeper locations, even if located under higher productivity surface waters.

[46] In both regions the CAR:BAR ratios increased significantly during the E/O transition. The increase in rain ratio (as reflected by higher CAR:BAR ratios) at the E/O boundary, regardless of causal mechanism, would imply a decreased drawdown of atmospheric CO₂ potentially providing a negative feedback to decreasing CO₂ at the boundary.

[47] This, interpretation, however, is not consistent with most records and with modeling results that indicate lower atmospheric pCO₂ at the E/O boundary [DeConto and Pollard, 2003; Pagani et al., 2005; Liu et al., 2009]. Perhaps, the effect of CaCO₃:C_{org} rain ratio changes on atmospheric pCO₂ are buffered through the coupled ballasting of C_{org} and CaCO₃ to depth [see Ridgwell, 2003; Thomas, 2007]. However, if our sedimentary records (i.e., CAR:BAR ratios) are representative of the rain ratio, then regardless of the absolute intensity of these changes on pCO₂ (i.e., buffered or not), the observed changes at the E/O are consistent with a negative feedback to decreasing atmospheric pCO₂. Therefore, our results preclude a change in the CaCO₃:C_{org} rain ratio as a cause for the low pCO₂ at this time. Indeed, this is consistent with modeling results that indicate that changes in C_{org} burial or changes in siliceous versus CaCO₃ export production (reflecting the rain ratio) are not consistent with observed changes in CCD and δ¹³C records [Merico et al., 2008].

[48] C_{org} burial in the sediment and BAR could be decoupled. High export production as indicated by high BARs may not represent high C_{org} burial due to mineralization of organic matter in deep water and at the sediment water

interface after burial [Olivarez Lyle and Lyle, 2006]. This decoupling would reduce the effect of CaCO₃:C_{org} rain ratio changes on pCO₂, at least on long (million years) time scales. Similarly, the higher burial of C (as CaCO₃) in marine sediments over longer time scales may ultimately remove C from the surface ocean-atmosphere system also impacting climate. Either way, our data suggests that other pCO₂ sinks were more effective during this transition, including possibly increased silicate weathering [Zachos et al., 1999; Ravizza and Peucker-Ehrenbrink, 2003; Zachos and Kump, 2005] and/or increased diatom productivity in the Southern Ocean.

5. Conclusions

[49] The correspondence between changes in carbonate and barite ARs during the late Eocene and early Oligocene suggests that surface ocean processes responsible for changes in BAR (i.e., export production) were generally coeval with changes in CAR (e.g., changes in deep water chemistry and circulation) although the direction and magnitude of these changes varied. This indicates that related mechanisms influence both parameters, such as climatically induced changes in both deep (impacting CaCO₃ preservation) and surface (impacting nutrient distribution) ocean circulation patterns and/or meridional overturning. CAR:BAR values increased dramatically during the E/O boundary transition, suggesting an increase in the CaCO₃:C_{org} rain ratio. These results indicate that export productivity changes in the equatorial and North Pacific did not contribute significantly to the lowering of pCO₂ at the E/O boundary. The increase in the CaCO₃:C_{org} rain ratio may have contributed to an increase in pCO₂ and could explain the abrupt recovery in pCO₂ to pre-transition values prior to a more gradual decline in pCO₂ at this time as suggested by high resolution reconstructions of atmospheric pCO₂ using B isotopes [Pearson et al., 2009].

[50] **Acknowledgments.** We would like to thank Bob Jones and Ellen Gray for help with laboratory work and constructive discussion. This work was funded by JOI-NSF grants OCE-9905362 and OCE-0352756 to A.P. M.C. was supported by an AMC student fellowship, E.G. was supported in part by NSF graduate research fellowship. M.L. and A.O.-L. were supported by NSF grant OCE-07253011. E.G. and M.C. contributed equally to the manuscript; each worked on samples from a different Leg.

References

- Anderson, L. D., and M. L. Delaney (2005), Middle Eocene to early Oligocene paleoceanography from Agulhas Ridge, Southern Ocean (Ocean Drilling Program Leg 177, Site 1090), *Paleoceanography*, 20, PA1013, doi:10.1029/2004PA001043.
- Anderson, L. G., D. Dyrssen, and E. P. Jones (1990), An assessment of the transport of atmospheric CO₂ into the Arctic Ocean, *J. Geophys. Res.*, 95, 1703–1711, doi:10.1029/JC095iC02p01703.
- Archer, D. (1996), A data-driven model of the calcite lysocline, *Global Biogeochem. Cycles*, 10, 511–526, doi:10.1029/96GB01521.
- Averyt, K. B., and A. Paytan (2004), A comparison of multiple proxies for export production in the equatorial Pacific, *Paleoceanography*, 19, PA4003, doi:10.1029/2004PA001005.
- Averyt, K. B., M. Calhoun, L. Schmalz, and A. Paytan (2005), Data report: Carbonate and barite trends across the Eocene/Oligocene boundary at Shatsky Rise, ODP Leg 198, *Proc. Ocean Drill. Program Sci. Results*, 198, 1–16, doi:10.2973/odp.proc.sr.198.106.2005.
- Bains, S., R. D. Norris, R. M. Corfield, and K. L. Faul (2000), Termination of global warmth at the Paleocene/Eocene boundary through productivity feedback, *Nature*, 407, 171–174, doi:10.1038/35025035.
- Barron, J. A., K. A. Nigrini, A. Pujos, T. Saito, F. Theyer, E. Thomas, and N. Weinreich (1985), Synthesis of central equatorial Pacific DSDP Leg 85 bio-stratigraphy: Refinement of Oligocene to recent biostratigraphy, *Initial Rep. Deep Sea Drill. Proj.*, 85, 905–934, doi:10.2973/dsdp.proc.85.130.1985.
- Berelson, W. (2001), POC fluxes into the ocean interior: A comparison of 4 US-JGOFS regional studies, *Oceanography*, 14, 59–67.
- Berggren, W. A., and D. R. Prothero (1992), Eocene-Oligocene climatic and biotic evolution: An overview, in *Eocene-Oligocene Climatic and Biotic Evolution*, edited by D. R. Prothero and W. A. Berggren, pp. 1–28, Princeton Univ. Press, Princeton, N. J.
- Berggren, F. C., D. V. Kent, C. C. Swisher III, and M.-P. Aubry (1995), A revised Cenozoic geochronology and chronostratigraphy, in *Geochronology, Time Scales, and Global Stratigraphic Correlation*, edited by W. A. Berggren et al., *Spec. Publ. SEPM Soc. Sediment. Geol.*, 54, 129–212.
- Bohaty, S. M., and J. C. Zachos (2003), A significant Southern Ocean warming event in the

- late middle Eocene, *Geology*, *31*, 1017–1020, doi:10.1130/G19800.1.
- Bohaty, S. M., J. C. Zachos, F. Florindo, and M. L. Delaney (2009), Coupled greenhouse warming and deep-sea acidification in the middle Eocene, *Paleoceanography*, *24*, PA2207, doi:10.1029/2008PA001676.
- Bonn, W. J., F. X. Gingele, H. Grobe, A. Mackensen, and D. K. Fütterer (1998), Palaeoproductivity at the Antarctic continental margin: Opal and barium records for the last 400 ka, *Palaeoogeogr. Palaeoclimatol. Palaeoecol.*, *139*, 195–211, doi:10.1016/S0031-0182(97)00144-2.
- Bralower, T. J. (2005), Data report: Paleocene-early Oligocene calcareous nannofossil biostratigraphy, ODP Leg 198 Sites 1209, 1210, and 1211 (Shatsky Rise, Pacific Ocean), *Proc. Ocean Drill. Program Sci. Results*, *198*, 1–15, doi:10.2973/odp.proc.sr.198.115.2005.
- Bralower, T. J., J. C. Zachos, E. Thomas, M. Parrow, C. K. Paull, D. C. Kelly, I. P. Silva, W. V. Sliter, and K. C. Lohmann (1995), Late Paleocene to Eocene paleoceanography of the equatorial Pacific Ocean: Stable isotopes recorded at Ocean Drilling Program Site 865, Allison Guyot, *Paleoceanography*, *10*, 841–865, doi:10.1029/95PA01143.
- Burgess, C. E., P. N. Pearson, C. H. Lear, H. E. G. Morgans, L. Handley, R. D. Pancost, and S. Schouten (2008), Middle Eocene climate cyclicity in the southern Pacific: Implications for global ice volume, *Geology*, *36*, 651–654, doi:10.1130/G24762A.1.
- Church, T. M. (1970), Marine barite, Ph.D. thesis, Univ. of Calif., San Diego.
- Coxall, H. K., P. A. Wilson, H. Pälike, C. H. Lear, and J. Backman (2005), Rapid stepwise onset of Antarctic glaciation and deeper calcite compensation in the Pacific Ocean, *Nature*, *433*, 53–57, doi:10.1038/nature03135.
- Cramer, B. S., J. R. Toggweiler, J. D. Wright, M. E. Katz, and K. G. Miller (2009), Ocean overturning since the Late Cretaceous: Inferences from a new benthic foraminiferal isotope compilation, *Paleoceanography*, *24*, PA4216, doi:10.1029/2008PA001683.
- Dean, W. E., J. V. Gardner, and D. A. Piper (1997), Inorganic geochemical indicators of glacial-interglacial changes in productivity and anoxia on the California continental margin, *Geochim. Cosmochim. Acta*, *61*, 4507–4518, doi:10.1016/S0016-7037(97)00237-8.
- de Boer, A. M., D. M. Sigman, J. R. Toggweiler, and J. L. Russell (2007), Effect of global ocean temperature change on deep ocean ventilation, *Paleoceanography*, *22*, PA2210, doi:10.1029/2005PA001242.
- DeConto, R. M., and D. Pollard (2003), Rapid Cenozoic glaciations of Antarctica induced by declining atmospheric CO₂, *Nature*, *421*, 245–249, doi:10.1038/nature01290.
- Diester-Haass, L. (1995), Middle Eocene to early Oligocene paleoceanography of the Antarctic Ocean (Maud Rise, ODP Leg 13, Site 689): Change from a low to a high productivity ocean, *Palaeoogeogr. Palaeoclimatol. Palaeoecol.*, *113*, 311–334, doi:10.1016/0031-0182(95)00067-V.
- Diester-Haass, L. (1996), Late Eocene–Oligocene paleoceanography in the southern Indian Ocean (ODP Site 744), *Mar. Geol.*, *130*, 99–119, doi:10.1016/0025-3227(95)00128-X.
- Diester-Haass, L., and R. Zahn (1996), Eocene–Oligocene transition in the Southern Ocean: History of water mass circulation and biological productivity, *Geology*, *24*, 163–166, doi:10.1130/0091-7613(1996)024<0163:EOTITS>2.3.CO;2.
- Diester-Haass, L., and R. Zahn (2001), Paleoproductivity increase at the Eocene–Oligocene climatic transition: ODP/DSDP sites 763 and 592, *Palaeoogeogr. Palaeoclimatol. Palaeoecol.*, *172*, 153–170, doi:10.1016/S0031-0182(01)00280-2.
- Dymond, J., J. B. Corliss, and R. Stilling (1976), Chemical composition and metal accumulation rates of metalliferous sediments from Sites 319, 320, and 321, *Initial Rep. Deep Sea Drill. Proj.*, *34*, 575–588.
- Dymond, J., E. Suess, and M. Lyle (1992), Barium in deep-sea sediment: A geochemical proxy for paleoproductivity, *Paleoceanography*, *7*, 163–181, doi:10.1029/92PA00181.
- Eagle, M., A. Paytan, K. R. Arrigo, G. van Dijken, and R. W. Murray (2003), A comparison between excess barium and barite as indicators of carbon export, *Paleoceanography*, *18*(1), 1021, doi:10.1029/2002PA000793.
- Edgar, K. M., P. A. Wilson, P. F. Sexton, and Y. Suganuma (2007), No extreme bipolar glaciations during the main Eocene calcite compensation shift, *Nature*, *448*, 908–911, doi:10.1038/nature06053.
- Eldrett, J. S., D. R. Greenwood, I. C. Harding, and M. Huber (2009), Increased seasonality through the Eocene to Oligocene transition in northern high latitudes, *Nature*, *459*, 969–973, doi:10.1038/nature08069.
- Emanuel, K. (2002), A simple model of multiple climate regimes, *J. Geophys. Res.*, *107*(D9), 4077, doi:10.1029/2001JD001002.
- Ewing, J., M. Ewing, T. Aitken, and W. J. Ludwig (1968), North Pacific sediment layers measured by seismic profiling, in *The Crust and Upper Mantle of the Pacific Area*, *Geophys. Monogr. Ser.*, vol. 12, edited by L. Knopoff, C. L. Drake, and P. J. Hart, pp. 147–173, AGU, Washington, D. C.
- Falkowski, P. G., M. E. Katz, A. H. Knoll, A. Quigg, J. A. Raven, O. Schofield, and F. J. R. Taylor (2004), The evolution of modern eukaryotic phytoplankton, *Science*, *305*, 354–360, doi:10.1126/science.1095964.
- Finkel, Z. V., M. E. Katz, J. D. Wright, O. M. Schofield, and P. G. Falkowski (2005), Climatically driven macroevolutionary patterns in the size of marine diatoms over the Cenozoic, *Proc. Natl. Acad. Sci. U. S. A.*, *102*, 8927–8932, doi:10.1073/pnas.0409907102.
- Frenz, M., R. Henrich, and B. Zychla (2006), Carbonate preservation patterns at the Ceará Rise—Evidence for the Pliocene super conveyor, *Mar. Geol.*, *232*, 173–180, doi:10.1016/j.margeo.2006.07.006.
- Gonneea, M. E., and A. Paytan (2006), Phase associations of barium in marine sediments, *Mar. Chem.*, *100*, 124–135, doi:10.1016/j.marchem.2005.12.003.
- Hollis, C. J., et al. (2009), Tropical sea temperatures in the high-latitude South Pacific during the Eocene, *Geology*, *37*, 99–102, doi:10.1130/G25200A.1.
- Huber, M., and R. Caballero (2003), Eocene El Niño: Evidence for robust tropical dynamics in the “hothouse,” *Science*, *299*, 877–881, doi:10.1126/science.1078766.
- Jaccard, S. L., G. H. Haug, D. M. Sigman, T. F. Pedersen, H. R. Thierstein, and U. Röhl (2005), Glacial/interglacial changes in subarctic North Pacific stratification, *Science*, *308*, 1003–1006, doi:10.1126/science.1108696.
- Katz, M. E., K. G. Miller, J. D. Wright, B. S. Wade, J. V. Browning, B. S. Cramer, and Y. Rosenthal (2008), Stepwise transition from the Eocene greenhouse to the Oligocene icehouse, *Nat. Geosci.*, *1*, 329–334, doi:10.1038/ngeo179.
- Kennett, J. P., and L. D. Stott (1990), Proteus and proto-oceanus: Ancestral Paleogene oceans as revealed from Antarctic stable isotopic results—ODP Leg 113, *Proc. Ocean Drill. Program Sci. Results*, *113*, 865–880.
- Lear, C. H., T. R. Bailey, P. N. Pearson, H. K. Coxall, and Y. Rosenthal (2008), Cooling and ice growth across the Eocene–Oligocene transition, *Geology*, *36*, 251–254, doi:10.1130/G24584A.1.
- Liu, Z., M. Pagani, D. Zinniker, R. DeConto, M. Huber, H. Brinkhuis, S. R. Shah, R. M. Leckie, and A. Pearson (2009), Global cooling during the Eocene–Oligocene climate transition, *Science*, *323*, 1187–1190, doi:10.1126/science.1166368.
- Lyle, M., A. Olivarez Lyle, J. Backman, and A. Tripathi (2005), Biogenic sedimentation in the Eocene equatorial Pacific: The stuttering greenhouse and Eocene carbonate compensation depth, *Proc. Ocean Drill. Program Sci. Results*, *199*, 1–35, doi:10.2973/odp.proc.sr.199.219.2005.
- Lyle, M., J. Barron, T. J. Bralower, M. Huber, A. Olivarez Lyle, A. C. Ravelo, D. K. Rea, and P. A. Wilson (2008), Pacific Ocean and Cenozoic evolution of climate, *Rev. Geophys.*, *46*, RG2002, doi:10.1029/2005RG000190.
- Marinov, I., and J. L. Sarmiento (2004), The role of the oceans in the global carbon cycle: An overview, in *The Ocean Carbon Cycle and Climate*, edited by M. Follows and T. Oguz, *NATO Sci. Ser., Ser. IV*, 251–295.
- Martin, J. H., G. A. Knauer, D. M. Karl, and W. W. Broenkow (1987), VERTEX: Carbon cycling in the northeast Pacific, *Deep Sea Res., Part A*, *34*, 267–285, doi:10.1016/0198-0149(87)90086-0.
- Martínez-Ruiz, F., A. Paytan, M. Kastner, J. M. González-Donosó, D. Linares, S. M. Bernasconi, and F. J. Jimenez-Espejo (2003), A comparative study of the geochemical and mineralogical characteristics of the S1 sapropel in the western and eastern Mediterranean, *Palaeoogeogr. Palaeoclimatol. Palaeoecol.*, *190*, 23–37, doi:10.1016/S0031-0182(02)00597-7.
- Merico, A., T. Tyrell, and P. A. Wilson (2008), Eocene/Oligocene ocean de-acidification linked to Antarctic glaciations by sea-level fall, *Nature*, *452*, 979–982, doi:10.1038/nature06853.
- Miller, K. G., and E. Thomas (1985), Late Eocene to Oligocene benthic foraminiferal isotopic record, Site 574, equatorial Pacific, *Initial Rep. Deep Sea Drill. Proj.*, *85*, 771–777, doi:10.2973/dsdp.proc.85.123.1985.
- Miller, K. G., R. G. Fairbanks, and G. S. Mountain (1987), Tertiary oxygen isotope synthesis, sea level history, and continental margin erosion, *Paleoceanography*, *2*, 1–19, doi:10.1029/PA002i001p00001.
- Miller, K. G., M. A. Kominz, J. V. Browning, J. D. Wright, G. S. Mountain, M. E. Katz, P. J. Sugarman, B. S. Cramer, N. Christie-Blick, and S. F. Pekar (2005a), The Phanerozoic record of global sea-level change, *Science*, *310*, 1293–1298, doi:10.1126/science.1116412.
- Miller, K. G., J. D. Wright, and J. V. Browning (2005b), Visions of ice sheets in a greenhouse world, *Mar. Geol.*, *217*, 215–231, doi:10.1016/j.margeo.2005.02.007.

- Miller, K. G., J. V. Browning, M.-P. Aubry, B. S. Wade, M. E. Katz, A. A. Kulpecz, and J. D. Wright (2008), Eocene-Oligocene global climate and sea-level changes: St. Stephens Quarry, Alabama, *Geol. Soc. Am. Bull.*, *120*, 34–53, doi:10.1130/B26105.1.
- Monnin, C., and D. Cividini (2006), The saturation state of the world's ocean with respect to (Ba, Sr)SO₄ solid solutions, *Geochim. Cosmochim. Acta*, *70*, 3290–3298, doi:10.1016/j.gca.2006.04.002.
- Monnin, C., C. Jeandel, T. Cattaldo, and F. Dehairs (1999), The marine barite saturation state of the world's oceans, *Mar. Chem.*, *65*, 253–261, doi:10.1016/S0304-4203(99)00016-X.
- Moore, T. C., Jr., J. Backman, I. Raffi, C. Nigrini, A. Sanfilippo, H. Pälike, and M. Lyle (2004), Paleogene tropical Pacific: Clues to circulation, productivity, and plate motion, *Paleoceanography*, *19*, PA3013, doi:10.1029/2003PA000998.
- Moore, T. C., Jr., R. D. Jarrard, A. Olivarez Lyle, and M. Lyle (2008), Eocene biogenic silica accumulation rates at the Pacific equatorial divergence zone, *Paleoceanography*, *23*, PA2202, doi:10.1029/2007PA001514.
- Nürnberg, C. C., G. Bohrmann, M. Schlüter, and M. Frank (1997), Barium accumulation in the Atlantic sector of the Southern Ocean: Results from 190,000-year records, *Paleoceanography*, *12*, 594–603, doi:10.1029/97PA01130.
- Olivarez Lyle, A., and M. W. Lyle (2006), Missing organic carbon in Eocene marine sediments: Is metabolism the biological feedback that maintains end-member climates?, *Paleoceanography*, *21*, PA2007, doi:10.1029/2005PA001230.
- Pagani, M., J. C. Zachos, K. H. Freeman, B. Tipler, and S. Bohaty (2005), Marked decline in atmospheric carbon dioxide concentrations during the Paleogene, *Science*, *309*, 600–603, doi:10.1126/science.1110063.
- Pälike, H., R. D. Norris, J. O. Herrle, P. A. Wilson, H. K. Coxall, C. H. Lear, N. J. Shackleton, A. K. Tripati, and B. S. Wade (2006), The heartbeat of the Oligocene climate system, *Science*, *314*, 1894–1898, doi:10.1126/science.1133822.
- Paytan, A., and E. M. Griffith (2007), Marine barite: Recorder of variations in ocean export productivity, *Deep Sea Res., Part II*, *54*, 687–705, doi:10.1016/j.dsr2.2007.01.007.
- Paytan, A., M. Kastner, and F. P. Chavez (1996), Glacial to interglacial fluctuations in productivity in the equatorial Pacific as indicated by marine barite, *Science*, *274*, 1355–1357, doi:10.1126/science.274.5291.1355.
- Pearson, P. N., B. E. van Dongen, C. J. Nicholas, R. D. Pancost, S. Schouten, J. M. Singano, and B. S. Wade (2007), Stable warm tropical climate through the Eocene epoch, *Geology*, *35*, 211–214, doi:10.1130/G23175A.1.
- Pearson, P. N., G. L. Foster, and B. S. Wade (2009), Atmospheric carbon dioxide through the Eocene-Oligocene climate transition, *Nature*, *461*, 1110–1113, doi:10.1038/nature08447.
- Pettrizzo, M. R., I. Premoli Silva, and P. Ferrari (2005), Data report: Paleogene planktonic foraminifer biostratigraphy, ODP Leg 198 Holes 1209A, 1210A, and 1211A (Shatsky Rise, northwest Pacific Ocean), *Proc. Ocean Drill. Program Sci. Results*, *198*, 1–56, doi:10.2973/odp.proc.sr.198.110.2005.
- Poag, C. W., E. Mankinen, and R. D. Norris (2003), Late Eocene impacts: Geologic record, correlation, and paleoenvironmental sequences, in *From Greenhouse to Icehouse: The Marine Eocene-Oligocene Transition*, edited by D. R. Prothero, L. C. Ivany, and E. Nesbitt, pp. 495–510, Columbia Univ. Press, New York.
- Prothero, D. R., L. C. Ivany, and E. A. Nesbitt (Eds.) (2003), *From Greenhouse to Icehouse: The Marine Eocene-Oligocene Transition*, 541 pp., Columbia Univ. Press, New York.
- Ravizza, G., and B. Peucker-Ehrenbrink (2003), The marine ¹⁸⁷Os/¹⁸⁸Os record of the Eocene-Oligocene transition: The interplay of weathering and glaciations, *Earth Planet. Sci. Lett.*, *210*, 151–165, doi:10.1016/S0012-821X(03)00137-7.
- Rea, D. K. and M. W. Lyle (2005), Paleogene calcite compensation depth in the eastern subtropical Pacific: Answers and questions, *Paleoceanography*, *20*, PA1012, doi:10.1029/2004PA001064.
- Ridgwell, A. J. (2003), An end to the “rain ratio” reign?, *Geochem. Geophys. Geosyst.*, *4*(6), 1051, doi:10.1029/2003GC000512.
- Rushdi, A. I., J. McManus, and R. W. Collier (2000), Marine barite and celestite saturation in seawater, *Mar. Chem.*, *69*, 19–31, doi:10.1016/S0304-4203(99)00089-4.
- Rutsch, H.-J., A. Mangini, G. Bonai, B. Dittrich-Hannen, P. W. Kubik, M. Suter, and M. Segl (1995), ¹⁰Be and Ba concentrations in West African sediments trace productivity in the past, *Earth Planet. Sci. Lett.*, *133*, 129–143, doi:10.1016/0012-821X(95)00069-0.
- Sarmiento, J. L., N. Gruber, M. A. Brzezinski, and J. P. Dunne (2004), High-latitude controls of thermocline nutrients and low latitude biological productivity, *Nature*, *427*, 56–60, doi:10.1038/nature02127.
- Sarnthein, M., K. Winn, J.-C. Duplessy, and M. R. Fontugne (1988), Global variations of surface ocean productivity in low and mid latitudes: Influence on CO₂ reservoirs of the deep ocean and atmosphere during the last 21,000 years, *Paleoceanography*, *3*, 361–399, doi:10.1029/PA003i003p00361.
- Scher, H. D., and E. E. Martin (2006), Timing and climatic consequences of the opening of Drake Passage, *Science*, *312*, 428–430, doi:10.1126/science.1120044.
- Schmitz, B. (1987), Barium, equatorial high productivity, and the northward wandering of the Indian continent, *Paleoceanography*, *2*, 63–77, doi:10.1029/PA002i001p00063.
- Scholl, D. W., A. J. Stevenson, M. A. Noble, and D. R. Rea (2003), The Meiji Drift body and Late Paleogene-Neogene paleoceanography of the North Pacific and Bering Sea region, in *From Greenhouse to Icehouse: The Marine Eocene-Oligocene Transition*, edited by D. R. Prothero, L. C. Ivany, and E. Nesbitt, pp. 119–153, Columbia Univ. Press, New York.
- Schumacher, S., and D. Lazarus (2004), Regional differences in pelagic productivity in the late Eocene to early Oligocene—A comparison of southern high latitudes and lower latitudes, *Palaeogeogr. Palaeoclimatol. Palaeoecol.*, *214*, 243–263.
- Shipboard Scientific Party (1985), Site 574, *Initial Rep. Deep Sea Drill. Proj.*, *85*, 225–329, doi:10.2973/dsdp.proc.85.105.1985.
- Shipboard Scientific Party (2002a), Leg 198 summary, *Proc. Ocean Drill. Program Initial Rep.*, *198*, 1–148, doi:10.2973/odp.proc.ir.198.191.2002.
- Shipboard Scientific Party (2002b), Site 1218, *Proc. Ocean Drill. Program Initial Rep.*, *199*, 1–126, doi:10.2973/odp.proc.ir.199.111.2002.
- Snoeckx, H., and D. Rea (1994), Dry bulk density and CaCO₃ relationships in upper Quaternary sediments of the eastern equatorial Pacific, *Mar. Geol.*, *120*, 327–333, doi:10.1016/0025-3227(94)90065-5.
- Srifer, R. L., and M. Huber (2007), Observational evidence for an ocean heat pump induced by tropical cyclones, *Nature*, *447*, 577–580, doi:10.1038/nature05785.
- Theyer, F., L. A. Mayer, J. A. Barron, and E. Thomas (1985), The equatorial Pacific high-productivity belt: Elements for a synthesis of Deep Sea Drilling Project Leg 85 results, *Initial Rep. Deep Sea Drill. Proj.*, *85*, 971–985, doi:10.2973/dsdp.proc.85.133.1985.
- Thomas, E. (2007), Cenozoic mass extinctions in the deep sea: What disturbs the largest habitat on Earth?, in *Large Ecosystem Perturbations: Causes and Consequences*, edited by S. Monechi, R. Coccioni, and M. Rampino, *Spec. Pap. Geol. Soc. Am.*, *424*, 1–23, doi:10.1130/2007.2424(01).
- Thomas, E., H. Brinkhuis, M. Huber, and U. Röhl (2006), An ocean view of the early Cenozoic greenhouse world, *Oceanography*, *19*, 63–72.
- Tripati, A., and E. Elderfield (2005), Deep-sea temperature and circulation changes at the Paleocene-Eocene thermal maximum, *Science*, *308*, 1894–1898, doi:10.1126/science.1109202.
- Van Andel, T. H. (1975), Mesozoic/Cenozoic calcite compensation depth and the global distribution of calcareous sediments, *Earth Planet. Sci. Lett.*, *26*, 187–194, doi:10.1016/0012-821X(75)90086-2.
- Wei, W. (1991), Evidence for an earliest Oligocene abrupt cooling in the surface waters of the Southern Ocean, *Geology*, *19*, 780–783, doi:10.1130/0091-7613(1991)019<0780:EFAEAO>2.3.CO;2.
- Wunsch, C., and R. Ferrari (2004), Vertical mixing, energy, and the general circulation of the oceans, *Annu. Rev. Fluid Mech.*, *36*, 281–314, doi:10.1146/annurev.fluid.36.050802.122121.
- Zachos, J. C., and L. R. Kump (2005), Carbon cycle feedbacks and the initiation of Antarctic glaciations in the earliest Oligocene, *Global Planet. Change*, *47*, 51–66, doi:10.1016/j.gloplacha.2005.01.001.
- Zachos, J. C., J. R. Breza, and S. W. Wise (1992), Early Oligocene ice-sheet expansion on Antarctica: Stable isotope and sedimentological evidence from Kerguelen Plateau, southern Indian Ocean, *Geology*, *20*, 569–573, doi:10.1130/0091-7613(1992)020<0569:EOISEO>2.3.CO;2.
- Zachos, J. C., L. D. Stott, and K. C. Lohmann (1994), Evolution of Early Cenozoic marine temperatures, *Paleoceanography*, *9*, 353–387, doi:10.1029/93PA03266.
- Zachos, J. C., T. M. Quinn, and K. A. Salamy (1996), High-resolution (10⁴ years) deep-sea foraminiferal stable isotope records of the Eocene-Oligocene climate transition, *Paleoceanography*, *11*, 251–266, doi:10.1029/96PA00571.
- Zachos, J. C., B. N. Opdyke, T. M. Quinn, C. E. Jones, and A. N. Halliday (1999), Eocene-Oligocene climate and seawater ⁸⁷Sr/⁸⁶Sr:

Is there a link?, *Chem. Geol.*, *161*, 165–180, doi:10.1016/S0009-2541(99)00085-6.

Zachos, J. C., M. Pagani, L. Sloan, E. Thomas, and K. Billups (2001), Trends, rhythms, and aberrations in global climate 65 ma to present, *Science*, *292*, 686–693, doi:10.1126/science.1059412.

Zachos, J. C., et al. (2005), Rapid acidification of the ocean during the Paleocene-Eocene thermal maximum, *Science*, *308*, 1611–1615, doi:10.1126/science.1109004.

Zanazzi, A., M. J. Kohn, B. J. MacFadden, and D. O. Terry Jr. (2007), Large temperature drop

across the Eocene-Oligocene transition in central North America, *Nature*, *445*, 639–642, doi:10.1038/nature05551.

K. Averyt, NOAA Earth System Research Laboratory, University of Colorado at Boulder, Boulder, CO 80305, USA.

T. Bralower, Department of Geosciences, Pennsylvania State University, University Park, PA 16802, USA.

M. Calhoun, A. Erhardt, and A. Paytan (corresponding author), Institute of Marine

Sciences, University of California, Santa Cruz, CA 95064, USA. (apaytan@ucsc.edu)

E. Griffith, Department of Geology, Kent State University, Kent, OH 44242, USA.

M. Lyle and A. Olivarez-Lyle, Department of Oceanography, Texas A&M University, College Station, TX 77843, USA.

E. Thomas, Department of Earth and Environmental Sciences, Wesleyan University, Middletown, CT 06459, USA.